Research Article

Ayse Kocak*, Duygu Harmancı, Merih Birlik, Sulen Sarıoglu, Osman Yılmaz, Zahide Cavdar and Gul Guner

Effects of epigallocatechin-3-gallate (EGCG) on a scleroderma model of fibrosis

Epigallokateşin-3-gallat'ın (EGCG) Skleroderma Fibrozis Modeli Üzerine Etkileri

https://doi.org/10.1515/tjb-2017-0185
Received April 6, 2017; accepted April 11, 2017; previously published online February 6, 2018

Abstract

Objective: The aim of the present study was to evaluate the potential protective effects of epigallocatechin-3-gallate (EGCG) on fibrosis in bleomycin induced scleroderma model.

Materials and methods: Thirty-two healthy female Balb-c mice with the average body weight of 22±5 g were used in this study. The mice were randomly divided into four groups as control (n=8), Bleomycin (n=8), Bleomycin+EGCG (n=8) and EGCG (n=8). Skin tissue samples were collected to quantify matrix metalloproteinases (MMP-1, MMP-8, MMP-13), p-SMAD 2/3 and SMAD 2/3 in protein homogenates by western blotting. TGF-β1 expression was determined by real-time PCR. Immunohistopathological and histopathological examinations of skin tissues were also done.

Results: When measured with Masson Trichrome, EGCG treatment was found to decrease fibrosis in connective tissue compared to the BLM injected control. EGCG was decreased dermal fibrosis. Bleomycin+EGCG group showed a significant reduction in fibrosis at the dermal surface area using hematoxylin measurements compared with the BLM group. MMP-1, MMP-8 protein levels were increased and p-SMAD 2/3 protein level was decreased. TGF-β mRNA expression was decreased in the EGCG+BLM group compared with the BLM group.

Conclusion: These results suggest an antifibrotic role for EGCG.

Keywords: BLM induced Scleroderma; EGCG; Fibrosis; TGF-β; MMPs.

Özet

Amaç: Bu çalışmanın amacı, bleomisinle (BLM) oluşturulmuş skleroderma modelinde epigallokateşin-3-gallat'ın (EGCG) fibrozis üzerine olası koruyucu etkilerini değerlendirmektir.

Gereç ve Yöntem: Bu çalışmada ortalama vücut ağırlığı 22±5 g olan 32 adet sağlıklı dişi *Balb-c* fare kullanıldı. Fareler rastgele olarak; kontrol (n=8), Bleomisin (n=8), Bleomisin+EGCG (n=8) ve EGCG (n=8) olmak üzere dört gruba ayrıldı. p-SMAD 2/3, SMAD 2/3 ve matriks metalloproteinaz (MMP-1, MMP-8, MMP-13) proteinlerinin western blotting tayini için dermal doku örnekleri toplandı. TGF-β1 mRNA ekspresyonu qPCR ile belirlendi. Deri dokularında immünohistopatolojik ve histopatolojik incelemeler yapıldı.

Sonuçlar: Masson Trikrom boyama sonuçlarına göre, EGCG uygulanan grupta fibrozisin azaldığı gözlendi. Hematoksilen-eozin boyama sonuçlarına göre, Bleomisin+EGCG

***Corresponding author: Ayse Kocak,** Institute of Health Sciences, Department of Molecular Medicine, Dokuz Eylul University, Izmir, Turkey, e-mail: kocak.ayse@gmail.com.
http://orcid.org/0000-0002-1510-2937
Duygu Harmancı and Zahide Cavdar: Institute of Health Sciences, Department of Molecular Medicine, Dokuz Eylul University, Izmir, Turkey, e-mail: duyguharmanci@gmail.com (D. Harmancı), zahide.cavdar@deu.edu.tr (Z. Cavdar)
Merih Birlik: Faculty of Medicine, Internal Medicine, Division of Rheumatology, Dokuz Eylul University, Izmir, Turkey, e-mail: birlikm@gmail.com
Sulen Sarıoglu: Faculty of Medicine, Department of Medical Pathology, Dokuz Eylül University, Izmir, Turkey, e-mail: sulen.sarioglu@deu.edu.tr
Osman Yılmaz: Institute of Health Sciences, Department of Laboratory Animal Sciences, Dokuz Eylul University, Izmir, Turkey, e-mail: osman.yilmaz@deu.edu.tr
Gul Guner: Department of Biochemistry, Faculty of Medicine, Izmir University of Economics, Izmir, Turkey, e-mail: akdogan.gul@izmirekonomi.edu.tr

grubu ile BLM grubu karşılaştırıldığında EGCG uygulanan grupta fibrozis anlamlı ölçüde azaldı. EGCG uygulanan grupta MMP-1, MMP-8 protein düzeylerinin arttığı ve p-SMAD 2/3 protein düzeyinin azaldığı belirlendi. BLM ve BLM + EGCG grupları karşılaştırıldığında TGF-β mRNA ekspresyonunun EGCG uygulanan grupta azaldığı gözlendi.
Sonuç: Sklerodermada, EGCG antifibrotik bir rol oynamaktadır.

Anahtar sözcükler: BLM ile oluşturulmuş scleroderma; EGCG; Fibrozis; TGF-β; MMP'ler.

Introduction

Systemic scleroderma (SSc) is a complex disease with three main clinical features: excessive chronic matrix (ECM) accumulation, vascular damage and inflammation autoimmunity [1]. Although the pathogenesis is unclear, SSc is characterized by abnormal reshaping of connective tissues in the skin and internal organs, due to the overproduction of ECM, in particular that of collagen, by fibroblasts [2]. SSc is a very rare disease all around the world having a prevalence ranging from 50 to 300 cases per million. As with other autoimmune diseases, women are at higher risk than men [3–5]. Concerning the in vivo research, the bleomycin-induced experimental scleroderma mouse is the most widely used model for studying scleroderma, and it is the best model for studying the prevention or treatment of fibrosis [6]. Nevertheless, there is no therapy or cure for SSc or for reversing the fibrosis of the skin and internal organs. TGF-β/Smad 2-3 is one of the most important pathways in scleroderma. TGF-β promotes ECM synthesis, such as collagen type I or fibronectin, thereby altering the proteins of the cell matrix, and modulating the production of related proteins by its proteolytic activity [7]. In this disease, increased TGF-β signaling may span fibroproliferative and inflammatory subsets and lead to the progressive deposition of ECM, resulting in fibrosis [8]. The expression of α-smooth muscle actin (α-SMA) in fibroblasts are also very important for differentiation into myofibroblasts and it coincides with an increase in the process of cell proliferation [9].

Matrix metalloproteinases (MMPs) are important enzymes of breakdown for various ECM components. MMPs can be divided into subgroups such as collagenases, stromelysins, stromelysin-like MMPs, gelatinases, membrane-type MMPs, and other Matrix metalloproteinases. MMP-1 (interstitial collagenase-1) is effective in initiating degradation of interstitial collagen types I, II, and III [10]. MMP-8 (collagenase-2 or neutrophil collagenase) belongs to the collagenase family, which degrades various ECM proteins such as collagen type I [11]. MMP-13 (collagenase-3) is the interstitial collagenase which is elevated and positively correlated with pulmonary fibrosis [12].

Epigallocatechin-3-gallate (EGCG), the most abundant catechin, is the major effective component of green tea and has been shown to have beneficial health effects on skin [13, 14]. In liver fibrosis, EGCG was shown to inhibit proliferation of fibroblasts, to reduce collagen deposition and to upregulate the mitochondrial respiratory chain [15]. It has also been promising for being a source of new molecular therapies.

Animal models are used to provide clues and therapeutic interventions for human diseases. Bleomycin is often used as an anti-tumor agent for a lot of cancers, which is originally isolated from the fungus *Streptomyces verticillus* [16]. Recent studies showed that bleomycin upregulates collagen mRNA expression in human lung or dermal fibroblasts in in vivo models [17, 18]. Yamamato et al. established a mice model for scleroderma by local treatment of bleomycin via *subcutaneous* (*sc*) injections for 21 days [19–24].

In this study, we investigated the possible antifibrotic effects of EGCG in vivo in bleomycin-induced sclerotic mice. This study contributes to the knowledge of the potential use of EGCG as a treatment for fibrosis in SSc patients.

Materials and methods

The study protocol was reviewed and approved by Dokuz Eylül University Ethics Committee for Animal Research (Protocol No: 79/2012).

Animals

Skin fibrosis was induced in 6–8-week-old, weighing about 20–22 g, pathogen-free female *Balb/c* mice (DEU, Department of Experimental Animals) by local injection of bleomycin for 21 days [19, 23, 25]. The animals were kept under standard animal laboratory conditions: temperature of 20–22°C, humidity of 55–60%, photoperiod of 12:12 h light: dark cycle. They had free access to standard laboratory feed and water. All methods including the euthanasia procedure were conducted in accordance with Guide for Care and Use of Laboratory Animals, Institute for Laboratory Animal Research, National Institute of Health.

Experimental design

The experimental design was performed according to Yamamato et al. [19, 23, 25]. Bleomycin was used for scleroderma model (Onko Koçsel, Turkey). EGCG (Sigma-Aldrich, USA) and bleomycin solutions were prepared at 1 μg/1 μL concentration before the experiment. A total of 32 female *Balb/c* mice were used and randomly divided into 4 groups of 8 animals each, as follows:

1. Control group (n:8) was given *subcutaneous* (*sc*) saline (SF) once a day, *intraperitoneal* (*ip*) SF twice a week,
2. BLM group (n:8) was given 100 μL of BLM *sc* once a day, 100 μL of SF *ip* twice a week,
3. BLM + EGCG group (n:8) was given 100 μL of BLM *sc* once a day, 100 μL of EGCG *ip* twice a week,
4. EGCG group (n:8) was given 100 μL of SF *sc* once a day, 100 μL of ECCG *ip* twice a week.

After 21 days, the animals were sacrificed under ether anesthesia in sterile condition. The injected skin was removed and processed for analysis. Skin tissue samples were separated for immunohistochemistry, histochemistry, western blotting analyses and qPCR analysis.

Immunohistochemical and histological analyses

The injected sections of skin were fixed in 10% formalin and embedded in paraffin. Four micrometer (μm) sections were stained with hematoxylin and eosin for the determination of dermal thickness. For the analysis of connective tissue, Masson's trichrome staining was performed. Dermal thicknesses of the injected sections were analyzed with an Nikon Eclipse C1 microscope (Nikon, Japan) at 200-fold magnification and digitalized by Nikon DS-Fi2 camera. Dermal sections were measured (as μm) on 10 areas. In each series of experiments, the dermal thicknesses were evaluated statistically.

α-Smooth muscle actin (α-SMA) (Thermo, USA) was used for immunohistochemical analyses. Four micrometer sections were cut, baked at 60°C for 30 min, and cooled. Sections were deparaffinized and rehydrated through graded alcohols to water. Antigen retrieval was required and it was done as follows: Slides were placed in Tris-buffered saline with 0.1% Tween-20 and loaded onto a Ventana Autostainer (Roche, USA). Blocking was done and the primary antibody (Thermo Fisher Scientific, USA) was applied for 30 min at room temperature. A horseradish peroxidase (HRP) derived secondary antibody (Thermo Fisher Scientific, USA) was applied. Slides were washed with wash buffer, incubated with liquid diaminobenzidine tetrahydrochloride (DAB) substrate (Agilent Technologies, Dako, USA) for 7 min, and rinsed with water. They were counterstained for 2 min with hematoxylin (Agilent Technologies, Dako, USA), blued with wash buffer, rinsed with water, dehydrated, cleared, and coverslipped. α-SMA positive cells were counted on five areas. Images were visualized with a Nikon Eclipse C1 microscope (Nikon, Japan) at 200-fold magnification and digitalized by Nikon DS-Fi2 camera. In each series of experiments, α-SMA positive cells were counted and evaluated statistically.

Preparation of tissue extracts for western blotting and quantitative reverse transcriptase–polymerase chain reaction (RT-PCR) analysis

Skin tissues were prepared for the western blotting and qPCR analysis. Each sample was homogenated with the trizol reagent (Roche, USA) using TissueLyser II (Qiagene, USA). The homogenate was incubated for 5 min at room temperature. A 1:5 volume of chloroform was added, and the tube was vortexed and subjected to centrifugation at 12,000 g for 15 min. The aqueous phase was isolated, and the total RNA was precipitated by cold absolute ethanol. After centrifugation and washing, the total RNA was finally eluted in 20 μL of RNase, DNase free water. The quantity was characterized using a UV spectrophotometer (NanoDrop 8000, Thermo Scientific, USA). RNA was isolated from the homogenates. The isolated RNA had a 260/280 ratio of 1.9–2.1.

For the isolation of total protein the organic phase was obtained at the bottom of the tube as described above (12,000 *g* centrifigation/15 min) Isopropanol in 1% glycerol (Sigma Aldrich, USA) was added to bottom of the tube. This protein precipitate was washed three times with 0.3 M guanidine hydrochloride in 95% ethanol. In addition, the protein precipitate was dried and solubilized in 1% sodium dodecyl sulfate (SDS). To ensure maximum dissolution, the protein precipitate was incubated at 50°C with intermittent vortexing in 1% SDS. This produced a fairly good amount of protein. Total protein extracts were transferred to fresh tubes and stored at −80°C.

Detection of MMP-1, MMP-8, MMP-13 and pSMAD 2/3 by western blotting

The protein concentration was quantified using a bicinchoninic acid (BCA) protein assay kit (Thermo Pierce,

USA). A total 25 μg of protein was separated by SDS–polyacrylamide gel electrophoresis and transferred to a 0.45 μm pore size, Polyvinylidene difluoride (PVDF) membrane (Millipore, USA) which was then blocked for 1 h at room temperature using 5% skim milk/Tris buffered saline-Tween (TBST). The blots (For each MMP type, four blots-representing four experimental groups) were incubated overnight with a 1:1000 dilution of appropriate primary antibody in 5% skim milk/TBST. The following antibodies were used: Rabbit MMP-1, MMP-8, MMP-13 (ThermoFisher Scientific, USA) and total Smad 2/3, P-Smad 2/3 (Santa Cruz Biotechnology, USA). After the primary incubation, membranes were washed with TBST, the blots were incubated with the appropriate horseradish peroxidase–conjugated mouse anti-rabbit secondary antibody (Santa Cruz Biotechnology, USA).

The following steps involved the processing of beta actin in a similar way, to be further used for comparison with the intensity of the MMP bands:

After visualizing the bands, MMP-1, MMP-8 and MMP-13 membranes were stripped, [using a solution (Thermo, USA) to dissociate the appropriate antibody] and the remaining protein band was re-incubated for β-actin using a monoclonal antibody (Santa Cruz Biotechnology, USA).

For the analysis of Smad and p-Smad: p-Smad membrane (following visualation for p-Smad) was stripped [using a solution (Thermo, USA) to dissociate the appropriate antibody] and re-incubated for Smad 2/3 with the Smad 2/3 antibody.

All protein bands were visualized using enhanced chemiluminescence (ECL) (Millipore, USA) and were quantitated using Image-J, NIH Image densitometry software. Relative expressions of proteins were calculated using the ratios: MMP-1/β-actin, MMP-8/β-actin, MMP-13/β-actin and P-Smad 2-3/Smad 2-3 (Figure 6). All experiments were performed in triplicate and the western blotting images were presented as the representative of three images.

Detection of TGF-β1 mRNA levels by quantitative reverse transcriptase–polymerase chain reaction (RT-PCR)

First-strand cDNA was synthesized from 1 μg total RNA in 20 μL by reverse transcription using high capacity cDNA kit (Applied Biosystems, CA, USA) according to the manufacturer's instructions. Reverse transcription reaction consisted of 2 μL Oligo-dT (50 μM), 2 μL of 10× reverse transcriptase buffer, 0.8 μL of deoxynucleoside triphosphate (25 mM), 1 μL of RNase inhibitor (40 U/μL), 1 μL of MultiScribe Reverse Transcriptase (50 U/μL), and RNase free dH_2O, up to a final volume of 20 μL. The cDNA was then stored at –20°C for the gene expression study.

Real time quantitative PCR was performed to detect the gene expression of TGF-β1 in skin tissue using SYBR master mix (ThermoFisher Scientific, USA) at 95°C for 10 min, followed by 40 cycles of 95°C for 15 s and 60°C for 30 s and the reaction was performed on Roche Lightcycler (Roche, USA). GAPDH, mouse sequence 5′-AGGTCGGTGTGAACGGATTTG-3′ and reverse 5′-TGTAGACCATGTAGTTGAGGTCA-3′, was used as an internal control. The primers that were used are TGF-β1 mouse sequence Forward 5′-GCCTGAGTGGCTGTCTTTTGA-3′ and Reverse 5′-CTGTATTCCGTCTCCTTGGTTCA-3′.

A relative quantification was performed using the $2^{\Delta\Delta Ct}$ method [26, 27]. The experiments were performed in triplicate and were repeated twice.

Statistical analysis

Data were presented as means ± SD and for comparisons between the groups, ANOVA Sidak analysis of variance and for dual comparisons Mann-Whitney U-test were used. Statistical evaluations were performed using the SPSS package program, version 20.0 (IBM, USA). A p-value of <0.05 was considered to be statistically significant.

Results

Investigation of the effects of EGCG on the expression of antifibrotic molecules using histochemical and immunohistochemical staining

H&E and Masson Trichrome staining were performed and the histological examination of the skin tissues from the mice is shown in Figures 1 and 2. The dermal thicknesses in the bleomycin + EGCG injected mice was significantly lower than in the bleomycin injected mice respectively ($p < 0.05$, Figures 1 and 2). Alpha smooth muscle actin immunohistochemical staining score was lower in the BLM + EGCG injected mice than bleomycin injected mice ($p < 0.05$, Figures 3 and 4). EGCG shows inhibitory effect on fibrosis.

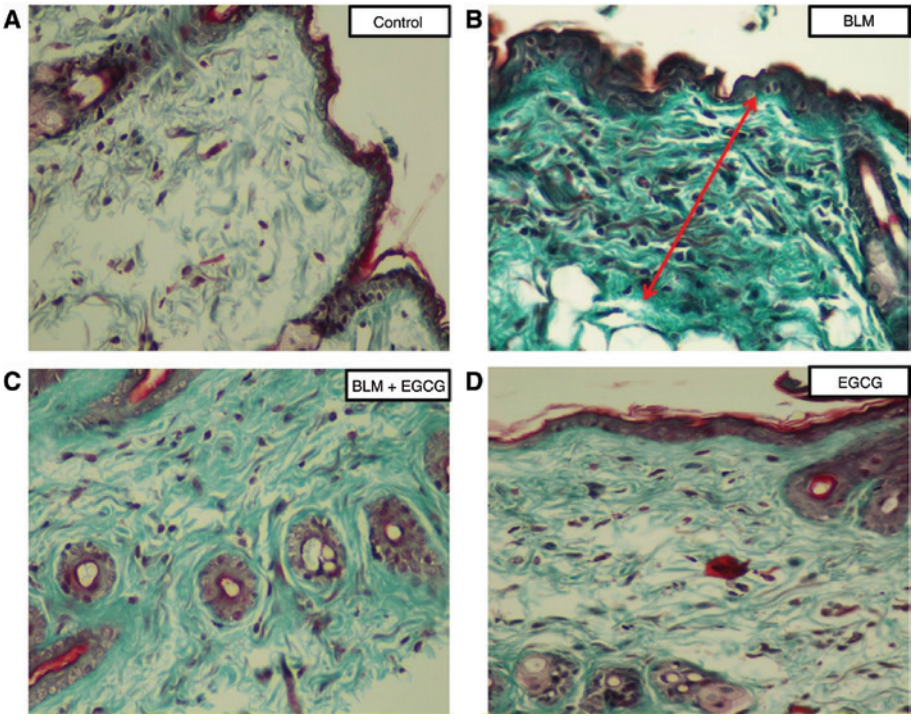

Figure 1: Masson-Trichrome staining.
Evidence of fibrosis (green color) was more prominent in the BLM group than BLM + EGCG group. Original magnification 20×. (A) Control group, (B) BLM group, (C) BLM + EGCG group, (D) EGCG group.

Effects of EGCG on MMP-1, MMP-8, MMP-13 and p-Smad2/3 protein expressions in skin tissues

As mentioned above, all experiments were performed in triplicate. For this reason, all images obtained from three independent western blotting experiments (MMP-1, MMP-8, MMP-13, p-smad 2/3) were evaluated statistically following the calculation of MMP(s)/β-Actin band area ratios obtained from densitometric measurements. The western blotting analysis showed that EGCG increased the MMP-1, MMP-8 levels in the bleomycin induced mice. Also, p-SMAD 2-3/Total SMAD 2-3 protein level ratio was decreased ($p < 0.05$, Figures 5 and 6) in the bleomycin + EGCG group. MMP-13 was not found to be significantly different in comparison with the BLM controls ($p > 0.05$, Figures 5 and 6).

Effect of EGCG on TGF-β1 mRNA levels in SSc tissues

As expected in a succesful bleomycin induced scleroderma model, the levels of TGF-β mRNAs in the BLM group was significantly increased ($p < 0.01$) compared with the control group. TGF-β mRNA levels in BLM + EGCG group was found to be lower ($p < 0.01$) in comparison with the BLM group (Figure 7).

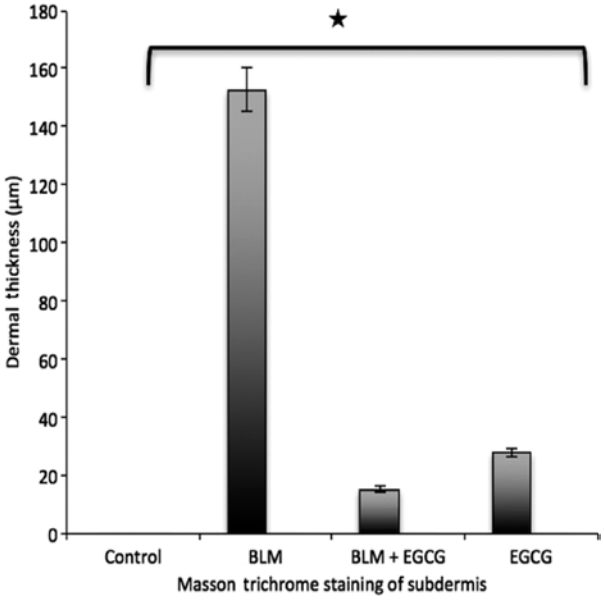

Figure 2: Staining score for Masson trichrome.
Results are presented as mean + SEM. *$p < 0.05$.

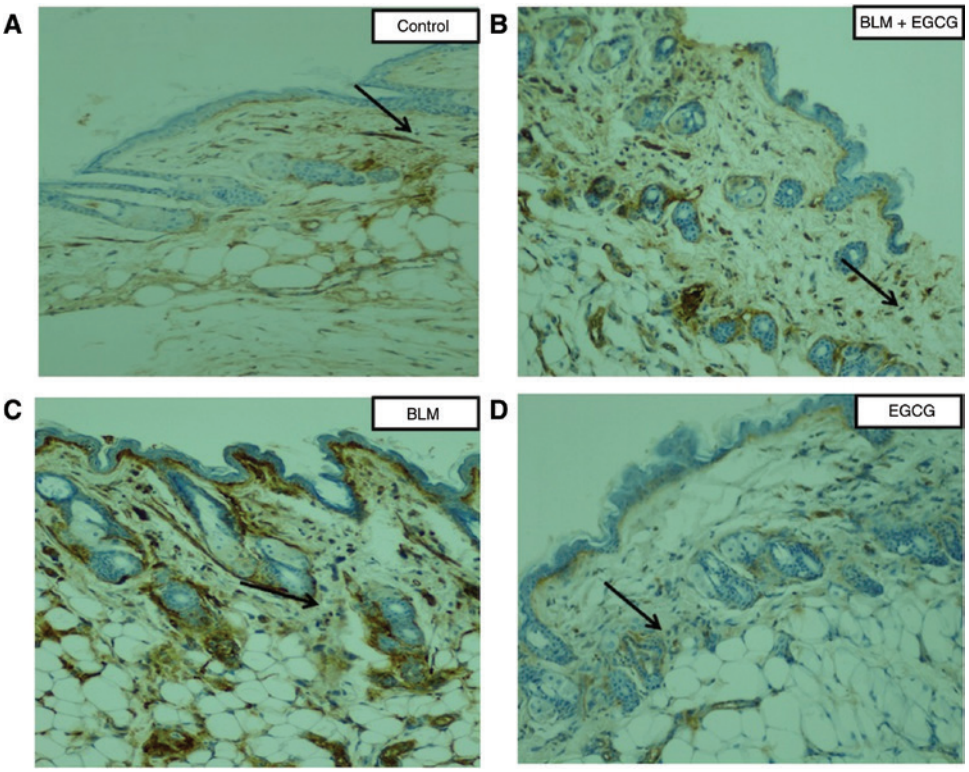

Figure 3: α-SMA staining of dermal tissue sections.
Alpha smooth muscle actin (α-SMA) is a marker for activated fibroblasts. The number of α-smooth muscle actin-positive fibroblast cells (black arrows) was higher in the BLM group than BLM + EGCG group. Original magnification 20×.

Discussion

Current treatment options for scleroderma have limitations that they simply control symptoms without targeting the underlying pathophysiology. More research is needed for these more feasible, safer treatment options. The investigation of the molecular mechanisms underlying scleroderma has attracted considerable attention in recent years [28]. It has been widely accepted that the dysregulation of the TGF-β/Smad pathway plays a key role in human skin tissues [29]. Although a variety of molecules have been investigated to check for possible antifibrotic effects of EGCG in pulmonary and hepatic fibrosis [30–32], there is no literature data encountered regarding the effect of EGCG on skin tissues in an experimental scleroderma model.

This is the first study aiming to elucidate if EGCG has an effect on the fibrotic component of scleroderma, in an experimental scleroderma model. We hypothesized that EGCG has an antifibrotic effect on scleroderma and the present study demonstrates for the first time that the natural green tea antioxidant, EGCG reduces collagens and TGF-β signaling and also, increases MMP-8, MMP-1 while decreasing p-SMAD 2/3 protein levels. Our results suggest that EGCG may be a potential candidate for therapeutic treatment by reducing the fibrotic effects of SSc disease characterized by oxidant stress as well as excessive collagen production and precipitation with fibroblasts in the skin.

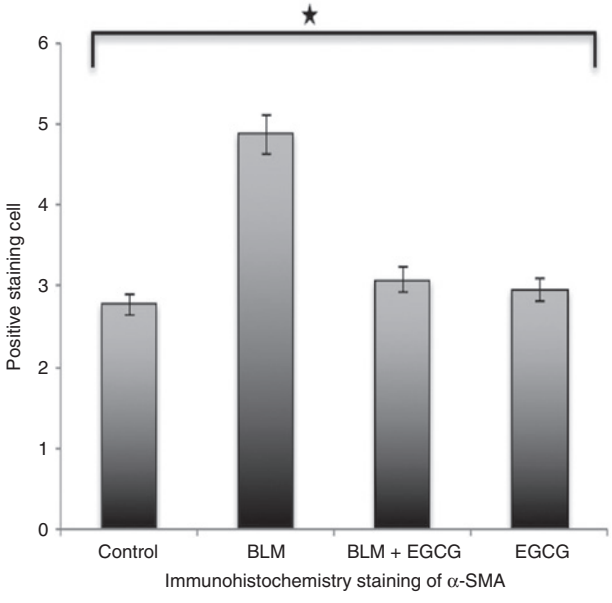

Figure 4: Staining score for alpha smooth muscle actin.
Results are presented as mean + SEM. *$p < 0.05$.

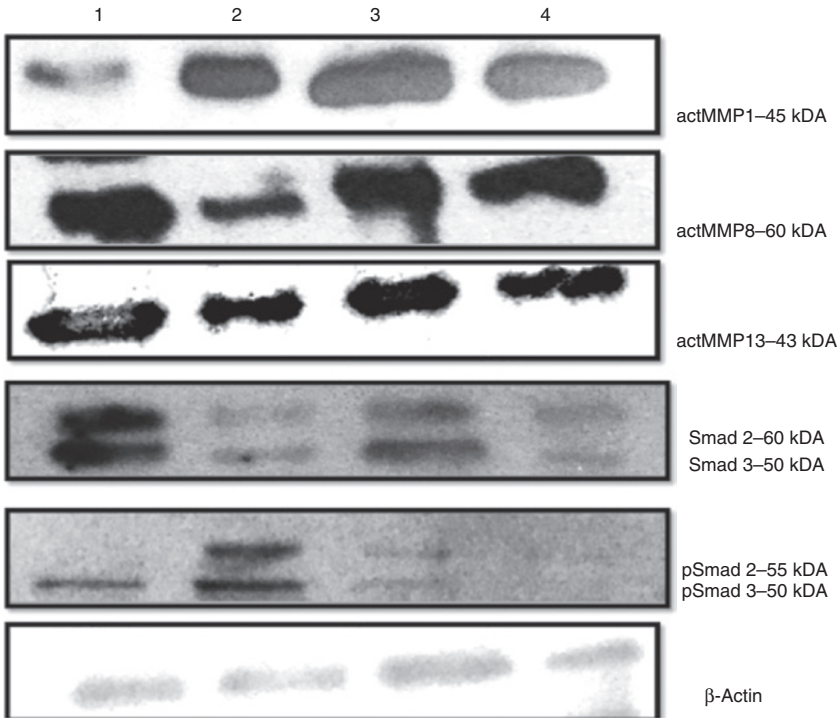

Figure 5: Effects of EGCG treatment on MMPs and Smad pathway proteins in scleroderma.
Western blottings were performed to measure protein levels of MMP1, MMP8, MMP13, SMAD 2/3 and pSMAD 2/3, as described under materials and methods. (1) Control group, (2) BLM group, (3) BLM + EGCG group, (4) EGCG group.

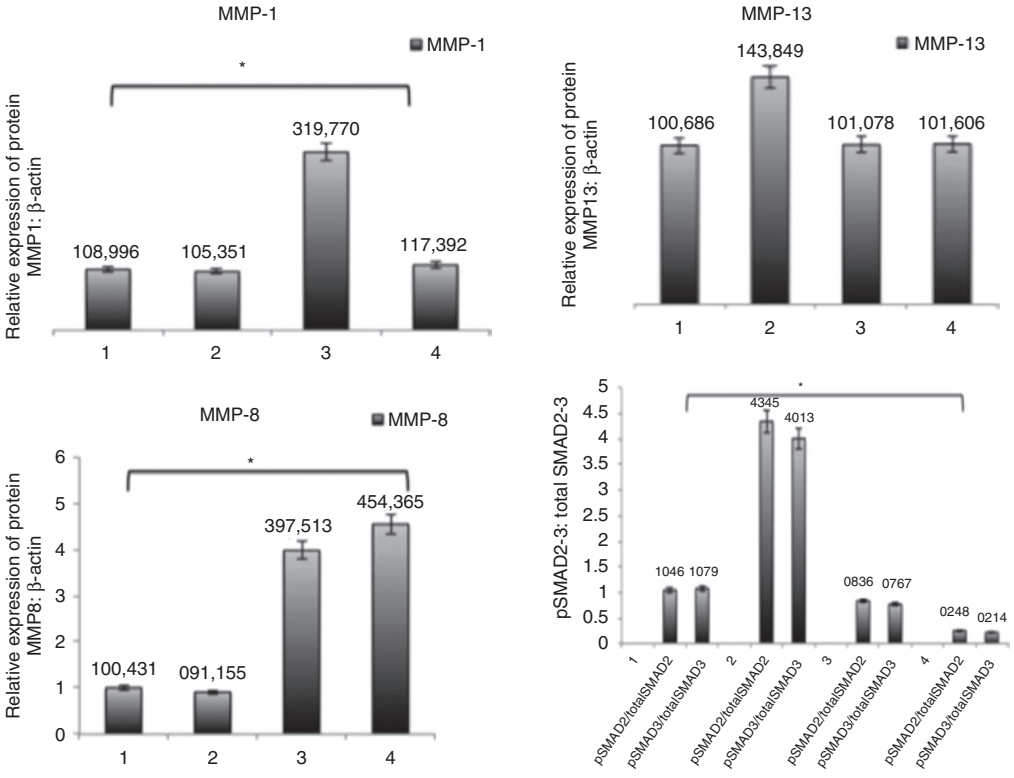

Figure 6: Effects of EGCG treatment on MMPs and Smad pathway proteins in scleroderma.
Quantitative representation of protein expression in all groups were obtained by densitometric analysis. (1) Control group, (2) BLM group, (3) BLM + EGCG group, (4) EGCG group. *$p < 0.05$.

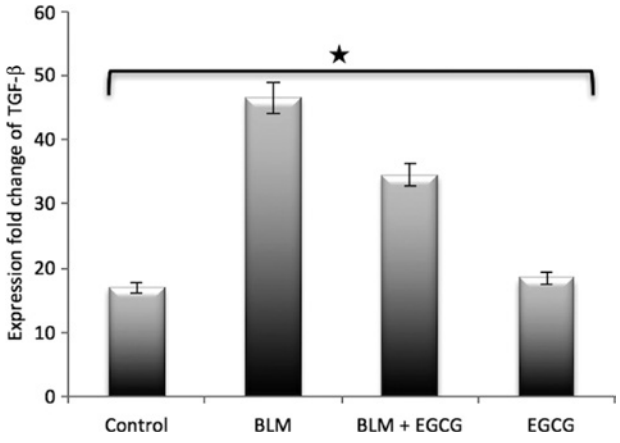

Figure 7: EGCG decreased TGF-β1 mRNA.
mRNA expression of TGF-β1 was analyzed by quantitative real-time qPCR. Results are presented as mean + SEM. *$p < 0.01$.

The most prominent clinical features of SSC are excessive accumulation of ECM components, especially type I and type III collagen, in related organs such as the skin and lung. In scleroderma fibroblasts, α-SMA, which is a marker of the myofibroblasts, shows increased expression. SSc is associated with the differentiation of fibroblasts into myofibroblasts, characterized by the expression of α-SMA contractile filaments. Myofibroblasts provide some activation features, including high levels of ECM gene expression, during normal repair or during pathological fibrotic procedures [33]. We also observed EGCG-induced inhibition of α-SMA expression in SSc groups. In addition, in our study, EGCG significantly decreased collagen levels in the EGCG treated groups. These findings indicate that EGCG inhibits production of collagen and the differentiation of fibroblasts.

There is important evidence in literature that EGCG modulates the ECM of different cell types [29]. EGCG has been shown to have anti-fibrotic, anti-cancer and anti-inflammatory activities via TGF-β and PDFG signaling in human and rat hepatic stellate cells, rat pancreatic cells, rat aortic smooth muscle cells and human keloid fibroblasts [34–40]. Hsieh et al. [41] observed that EGCG blocks the ability of TGF-β1 to produce collagen. Another study indicated that EGCG reduced myocardial fibrosis in vitro and in vivo [42]. Bleomycin induced, in rat lung fibroblast cultures, an increase in TGF-β mRNA synthesis and TGF-β protein, followed by increased procollagen gene transcription [43]. Increased expression of TGF-β1 and TGF-β2 mRNA were also detected in the lesional skin. In addition, recently, increased expression and synthesis of TGF-β1 in bleomycin-induced mice have been observed [44]. Dooley et al. [29] showed that EGCG can effectively inhibit fibroblast-mediated gel contraction. EGCG has shown an inbitory effect on human dermal fibroblasts [45]. Our data show, for the first time in the literature, the decreasing effects of EGCG on collagen, TGF-β and p-SMAD 2/3 mRNA levels in skin tissues of the bleomycine induced sclerodermic animals. In addition, we noted that MMP-1, MMP-8 protein levels in the scleroderma mice fibroblasts increased by treatment with EGCG. This observation suggests that EGCG may have dual effects on the metabolism of collagen in SSc, involving both inhibiting the production and increasing the degradation of collagen. In parallel in our results EGCG was shown to inhibit fibroblast activation and collagen accumulation by inhibiting TGF-β1 signaling and thus was considered to be effective on pulmonary fibrosis [46].

TGF-β is produced by fibroblasts and infiltrating cells at the sclerotic stage in the bleomycin model. In this model, TGF-β and phosphorylated Smad2/3 are upregulated [47]. EGCG is a powerful antioxidant which has a lot of health benefits. The effects may be due to its antioxidative action [48–50]. EGCG reduced the increase in α-SMA expression via TGF-β. These results indicate that the inhibitory effect of EGCG on α-SMA expression is independent of its antioxidative action. Tabuchi et al. [51] found that EGCG binds to the TGF-β receptor and affects collagen degradation by regulating MMPs. The effects of EGCG on scleroderma might thus be partially caused by inhibition of phosphorylation of Smad2/3.

Taking our results into consideration, we think that EGCG treatment, by inhibiting TGF-β1 signaling pathway, may partially revert differentiated myofibroblasts, which is supported by our data on decreased α-SMA.

In conclusion, our findings provide new evidence to medical literature, that EGCG reduces skin fibrosis by increasing MMP-1 and MMP-8. This study highlights the potential use of EGCG as a new drug for the treatment of fibrosis (following further investigations), in patients with SSc.

Acknowledgements: This research was supported by a grant supplied from Dokuz Eylul University Research Fund (2014.KB.SAG.024) and carried out at Dokuz Eylul University Medicine Faculty of Research Laboratory (R-LAB).

Conflict of interest statement: There are no conflicts of interest among the authors.

References

1. Varga J, Abraham D. Systemic sclerosis: a prototypic multisystem fibrotic disorder. J Clin Invest 2007;117:557–67.

2. Bhattacharyya S, Wei J, Varga J. Understanding fibrosis in systemic sclerosis: shifting paradigms, emerging opportunities. Nat Rev Rheumatol 2011;8:42–54.
3. Hunzelmann N, Genth E, Krieg T, Lehmacher W, Melchers I, Meurer M, et al. The registry of the German Network for Systemic Scleroderma: frequency of disease subsets and patterns of organ involvement. Rheumatology (Oxford) 2008;47:1185–92.
4. Allanore Y, Dieude P, Boileau C. Genetic background of systemic sclerosis: autoimmune genes take centre stage. Rheumatology (Oxford) 2010;49:203–10.
5. Mayes MD, Lacey JV Jr, Beebe-Dimmer J, Gillespie BW, Cooper B, Laing TJ, et al. Prevalence, incidence, survival, and disease characteristics of systemic sclerosis in a large US population. Arthritis Rheum 2003;48:2246–55.
6. Avouac J, Elhai M, Allanore Y. Experimental models of dermal fibrosis and systemic sclerosis. Joint Bone Spine 2013;80:23–8.
7. Roberts AB, Sporn MB. Transforming growth factors. Cancer Surv 1985;4:683–705.
8. Mahoney JM, Taroni J, Martyanov V, Wood TA, Greene CS, Pioli PA, et al. Systems level analysis of systemic sclerosis shows a network of immune and profibrotic pathways connected with genetic polymorphisms. PLoS Comput Biol 2015;11:e1004005.
9. Hinz B, Phan SH, Thannickal VJ, Galli A, Bochaton-Piallat ML, Gabbiani G, et al. The myofibroblast: one function, multiple origins. Am J Pathol 2007;170:1807–16.
10. Kahari VM, Saarialho-Kere U. Matrix metalloproteinases in skin. Exp Dermatol 1997;6:199–213.
11. Siller-López F, Sandoval A, Salgado S, Salazar A, Bueno M, Garcia J, et al. Treatment with human metalloproteinase-8 gene delivery ameliorates experimental rat liver cirrhosis. Gastroenterology 2004;126:1122–33; discussion 949.
12. Asano Y, Ihn H, Kubo M, Jinnin M, Mimura Y, Ashida R, et al. Clinical significance of serum levels of matrix metalloproteinase-13 in patients with systemic sclerosis. Rheumatology (Oxford) 2006;45:303–37.
13. Roh E, Kim JE, Kwon JY, Park JS, Bode AM, Dong Z, et al. Molecular mechanisms of green tea polyphenols with protective effects against skin photoaging. Crit Rev Food Sci Nutr 2017;57:1631–7.
14. White OP, Tribout H, Baron E. Protective mechanisms of green tea polyphenols in skin. Oxid Med Cell Longev 2012;2012:Article ID: 560682;8 pages.
15. Santamarina AB, Carvalho-Silva M, Gomes LM, Okuda MH, Santana AA, Streck EL, et al. Decaffeinated green tea extract rich in epigallocatechin-3-gallate prevents fatty liver disease by increased activities of mitochondrial respiratory chain complexes in diet-induced obesity mice. J Nutr Biochem 2015;26:1348–56.
16. Umezawa H, Maeda K, Takeuchi T, Okami Y. New antibiotics, bleomycin A and B. J Antibiot (Tokyo) 1966;19:200–9.
17. Yamamoto T, Eckes B, Krieg T. Bleomycin increases steady-state levels of type I collagen, fibronectin and decorin mRNAs in human skin fibroblasts. Arch Dermatol Res 2000;292:556–61.
18. Clark JG, Starcher BC, Uitto J. Bleomycin-induced synthesis of type I procollagen by human lung and skin fibroblasts in culture. Biochim Biophys Acta 1980;631:359–70.
19. Yamamoto T, Kuroda M, Nishioka K. Animal model of sclerotic skin. III: histopathological comparison of bleomycin-induced scleroderma in various mice strains. Arch Dermatol Res 2000;292:535–41.
20. Yamamoto T, Nishioka K. Animal model of sclerotic skin. IV: induction of dermal sclerosis by bleomycin is T cell independent. J Invest Dermatol 2001;117:999–1001.
21. Yamamoto T, Nishioka K. Animal model of sclerotic skin. V: increased expression of alpha-smooth muscle actin in fibroblastic cells in bleomycin-induced scleroderma. Clin Immunol 2002;102:77–83.
22. Yamamoto T, Nishioka K. Animal model of sclerotic skin. VI: evaluation of bleomycin-induced skin sclerosis in nude mice. Arch Dermatol Res 2004;295:453–6.
23. Yamamoto T, Takagawa S, Katayama I, Yamazaki K, Hamazaki Y, Shinkai H, et al. Animal model of sclerotic skin. I: local injections of bleomycin induce sclerotic skin mimicking scleroderma. J Invest Dermatol 1999;112:456–62.
24. Yamamoto T, Takahashi Y, Takagawa S, Katayama I, Nishioka K, et al. Animal model of sclerotic skin. II. Bleomycin induced scleroderma in genetically mast cell deficient WBB6F1-W/W(V) mice. J Rheumatol 1999;26:2628–34.
25. Yamamoto T. Animal model of sclerotic skin induced by bleomycin: a clue to the pathogenesis of and therapy for scleroderma? Clin Immunol 2002;102:209–16.
26. Shi R, Chiang VL. Facile means for quantifying microRNA expression by real-time PCR. Biotechniques 2005;39: 519–25.
27. Schmittgen TD, Livak KJ. Analyzing real-time PCR data by the comparative C(T) method. Nat Protoc 2008;3:1101–8.
28. Abraham DJ, Krieg T, Distler J, Distler O. Overview of pathogenesis of systemic sclerosis. Rheumatology (Oxford) 2009; 48(Suppl 3):iii3–7.
29. Dooley A, Shi-Wen X, Aden N, Tranah T, Desai N, Denton CP, et al. Modulation of collagen type I, fibronectin and dermal fibroblast function and activity, in systemic sclerosis by the antioxidant epigallocatechin-3-gallate. Rheumatology (Oxford) 2010;49:2024–36.
30. Sriram N, Kalayarasan S, Sudhandiran G. Epigallocatechin-3-gallate exhibits anti-fibrotic effect by attenuating bleomycin-induced glycoconjugates, lysosomal hydrolases and ultrastructural changes in rat model pulmonary fibrosis. Chem Biol Interact 2009;180:271–80.
31. Yasuda Y, Shimizu M, Sakai H, Iwasa J, Kubota M, Adachi S, et al. (–)-Epigallocatechin gallate prevents carbon tetrachloride-induced rat hepatic fibrosis by inhibiting the expression of the PDGFRβ and IGF-1R. Chem Biol Interact 2009;182: 159–64.
32. Zhen M, Wang Q, Huang X, Cao L, Chen X, Sun K, et al. Green tea polyphenol epigallocatechin-3-gallate inhibits oxidative damage and preventive effects on carbon tetrachloride-induced hepatic fibrosis. J Nutr Biochem 2007;18:795–805.
33. Desmouliere A, Chaponnier C, Gabbiani G. Tissue repair, contraction, and the myofibroblast. Wound Repair Regen 2005;13:7–12.
34. Chen A, Zhang L, Xu J, Tang J. The antioxidant (-)-epigallocatechin-3-gallate inhibits activated hepatic stellate cell growth and suppresses acetaldehyde-induced gene expression. Biochem J 2002;368(Pt 3):695–704.
35. Chen A, Zhang L. The antioxidant (-)-epigallocatechin-3-gallate inhibits rat hepatic stellate cell proliferation in vitro by blocking the tyrosine phosphorylation and reducing the gene expression of platelet-derived growth factor-beta receptor. J Biol Chem 2003;278:23381–9.

36. Nakamuta M, Higashi N, Kohjima M, Fukushima M, Ohta S, Kotoh K, et al. Epigallocatechin-3-gallate, a polyphenol component of green tea, suppresses both collagen production and collagenase activity in hepatic stellate cells. Int J Mol Med 2005;16:677–81.
37. Asaumi H, Watanabe S, Taguchi M, Tashiro M, Nagashio Y, Nomiyama Y, et al. Green tea polyphenol (-)-epigallocatechin-3-gallate inhibits ethanol-induced activation of pancreatic stellate cells. Eur J Clin Invest 2006;36:113–22.
38. Meng M, Li YQ, Yan MX, Kou Y, Ren HB. Effects of epigallocatechin gallate on diethyldithiocarbamate-induced pancreatic fibrosis in rats. Biol Pharm Bull 2007;30:1091–6.
39. Ahn HY, Hadizadeh KR, Seul C, Yun YP, Vetter H, Sachinidis A, et al. Epigallocathechin-3 gallate selectively inhibits the PDGF-BB-induced intracellular signaling transduction pathway in vascular smooth muscle cells and inhibits transformation of sis-transfected NIH 3T3 fibroblasts and human glioblastoma cells (A172). Mol Biol Cell 1999;10:1093–104.
40. Park G, Yoon BS, Moon JH, Kim B, Jun EK, Oh S, et al. Green tea polyphenol epigallocatechin-3-gallate suppresses collagen production and proliferation in keloid fibroblasts via inhibition of the STAT3-signaling pathway. J Invest Dermatol 2008;128:2429–41.
41. Hsieh YP, Chen HM, Lin HY, Yang H, Chang JZ. Epigallocatechin-3-gallate inhibits transforming-growth-factor-beta1-induced collagen synthesis by suppressing early growth response-1 in human buccal mucosal fibroblasts. J Formos Med Assoc 2017;116:107–13.
42. Lin CM, Chang H, Wang BW, Shyu KG. Suppressive effect of epigallocatechin-3-O-gallate on endoglin molecular regulation in myocardial fibrosis in vitro and in vivo. J Cell Mol Med 2016;20:2045–55.
43. Breen E, Shull S, Burne S, Absher M, Kelley J, Phan S, et al. Bleomycin regulation of transforming growth factor-beta mRNA in rat lung fibroblasts. Am J Respir Cell Mol Biol 1992;6:146–52.
44. Oi M, Yamamoto T, Nishioka K. Increased expression of TGF-beta1 in the sclerotic skin in bleomycin-'susceptible' mouse strains. J Med Dent Sci 2004;51:7–17.
45. Suzuki Y, Hattori S, Isemura M. Epigallocatechin-3-O-gallate inhibits fibroblast contraction of floating collagen gel: interaction between epigallocatechin-3-O-gallate and platelet derived growth factor. Biosci Biotechnol Biochem 2004;68:1817–20.
46. Sriram N, Kalayarasan S, Manikandan R, Arumugam M, Sudhandiran G. Epigallocatechin gallate attenuates fibroblast proliferation and excessive collagen production by effectively intervening TGF-beta1 signalling. Clin Exp Pharmacol Physiol 2015;42:849–59.
47. Takagawa S, Lakos G, Mori Y, Yamamoto T, Nishioka K, Varga J. Sustained activation of fibroblast transforming growth factor-beta/Smad signaling in a murine model of scleroderma. J Invest Dermatol 2003;121:41–50.
48. Nanjo F, Goto K, Seto R, Suzuki M, Sakai M, Hara Y. Scavenging effects of tea catechins and their derivatives on 1,1-diphenyl-2-picrylhydrazyl radical. Free Radic Biol Med 1996;21:895–902.
49. Nanjo F, Mori M, Goto K, Hara Y. Radical scavenging activity of tea catechins and their related compounds. Biosci Biotechnol Biochem 1999;63:1621–3.
50. Higdon JV, Frei B. Tea catechins and polyphenols: health effects, metabolism, and antioxidant functions. Crit Rev Food Sci Nutr 2003;43:89–143.
51. Tabuchi M, Hayakawa S, Honda E, Ooshima K, Itoh T, Yoshida K, et al. Epigallocatechin-3-gallate suppresses transforming growth factor-beta signaling by interacting with the transforming growth factor-beta type II receptor. World J Exp Med 2013;3:100–7.